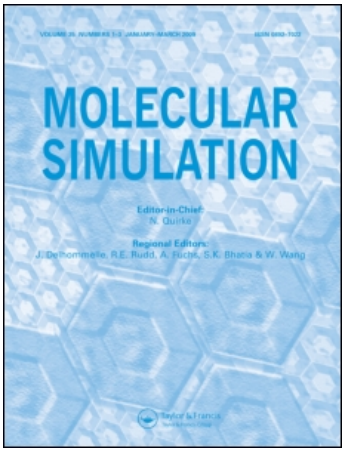

Molecular Simulation
Publication details, including instructions for authors and subscription information:
http://www.informaworld.com/smpp/title~content=t713644482

Properties of a Simple Polymer Chain in a Narrow Capillary—2 Dimensional Monte Carlo Study

Yoshimasa Yoshida[a]; Yasuaki Hiwatari[a]
[a] Department of Computational Science, Faculty of Science, Kanazawa University, Ishikawa, Japan

To cite this Article Yoshida, Yoshimasa and Hiwatari, Yasuaki(1999) 'Properties of a Simple Polymer Chain in a Narrow Capillary—2 Dimensional Monte Carlo Study', Molecular Simulation, 22: 2, 91 — 121
To link to this Article: DOI: 10.1080/08927029908022090
URL: http://dx.doi.org/10.1080/08927029908022090

Molecular Simulation, 1999, Vol. 22, pp. 91–121
Reprints available directly from the publisher
Photocopying permitted by license only

PROPERTIES OF A SIMPLE POLYMER CHAIN IN A NARROW CAPILLARY – 2 DIMENSIONAL MONTE CARLO STUDY

YOSHIMASA YOSHIDA* and YASUAKI HIWATARI

Department of Computational Science, Faculty of Science, Kanazawa University, Kanazawa, Ishikawa 920-1192, Japan

(Received October 1998; accepted October 1998)

In this paper, we have carried out Monte Carlo simulations of a single polymer chain confined in two parallel impenetrable adsorbing walls. Polymer moves obey the Bond-Fluctuation-Method and sampling of configurations obeys the Entropic-Sampling Method. We have investigated effects of both the number of monomers of a polymer under the constant wall distance condition and the wall distance at constant number of monomers. We obtained specific transitions and various physical properties in terms of the Helmholtz free energy and the specific heat *etc.*

Keywords: Linear polymer chain; capillary; free energy; radius of gyration; Entropic-Sampling Monte Carlo

1. INTRODUCTION

Polymers like biopolymers (*e.g.*, protein, nucleic acid), natural polymers (*e.g.*, raw rubber, starch), synthetic polymers (*e.g.*, nylon, polyethylene) and so on, are found everywhere and used in practical applications in many fields. Recently, polymers in a confined space become one of very interesting topics in statistical mechanics, and have important applications in industries.

For instance, apparatus for the separation and molecular weight determination based on capillary electrophoresis high performance, is useful for analyzing polymers such as peptides, proteins, DNA *etc.* [1–4].

* Corresponding author.

To improve the resolution *via* the molecular sieve effect, a gel (*e.g.*, polyacrylamide gel) is held in a capillary as a support [5–11]. Instead of the gel filled capillary, polymer melts are also used with the molecular sieve effect *e.g.*, derivative celluloses, non-crossed polyacrylamide melts for a buffer solution in a capillary [12–14]. The capillary is generally made of fused silica, fluororesin, or glass on account of the heat radiation effect. A problem in the process of making the capillary is to induce negative charges in its inner surface. The sampling solutions usually contain proteins in biomolecules, and proteins adsorb with these materials. Therefore, sampling analyses may be influenced by such adsorption effects. To cope with this situation, the chemical treatment of the adjustment of acidity (pH) and/or viscosity of the buffer solution [15] and the capillary inner surface improvement by the introduction of many hydrophilic groups through the siloxane bond (Si—O bond) [16] or the Si—C bond [17] have been used.

As an example of technical applications, there are polymer-matrix composite materials. These are divided into the fiber-reinforced type, laminate type, and particle filler type. For the fiber-reinforced polymer composite material, a fibrous component such as glass, Kevlar, graphite *etc.*, is embedded into an amorphous polymer matrix such as epoxies, polyesters, polyamides *etc.* The fiber component generally serves to reinforce the specific modulus and the specific strength of the mechanically weak polymer matrix, whereas the matrix determines the overall physico-chemical properties of the composite material. The fiber-reinforced composite materials with a combination of two components are lighter than the conventional ceramics or metallic materials while exhibiting comparable or even better thermal and mechanical properties. Therefore, these composite materials are extensively applied in the automotive, aerospace, and electronic industry as substitutes for ceramics or metals. The properties of these polymer-matrix composite materials are substantially determined by the interaction between the fiber and the polymer component at the interface [18–20].

In this paper, we investigate properties of a polymer chain in a narrow capillary that simulates a system in a confined space mentioned above. The paper is organized as follows; we describe the model used in the simulations and the techniques of the simulations in Section 2. Section 3 is the main part of this paper. In Subsection 3.1, in order to test the scaling property and to obtain the relation between a wall distance D and a number of monomers N, we first study an isolated linear polymer chain. Subsection 3.2 provides results of a number of monomers dependence for a fixed wall distance. In Subsection 3.3, in order to investigate influences of existance of one wall,

the simulation of a polymer near the wall in semi-confined space has been carried out. Subsection 3.4 presents results of the wall-distance dependence for a fixed number of monomers. Section 4 contains conclusions and discussions.

2. MODEL AND COMPUTATIONAL METHOD

Here we study a polymer chain in a very narrow confined space. Especially, we study the case of a system, in which a remarkable influence of capillary walls takes place. The model which we use is as follows.

In this paper, we consider a 2-dimensional lattice space. A single linear polymer chain is placed in between two parallel impenetrable walls. Walls are prepared in parallel to x-axis and perpendicular to y-axis. To be able to treat a polymer chain as realistic as possible, we take into consideration excluded volume interactions between monomers. We assume that the monomer-capillary walls interaction is a short-range attractive one, *i.e.*, if one monomer lies on the adsorbing capillary walls, it receives a negative energy cost $E = -u_0$ (where $u_0 > 0$ is used as a unit energy for our system).

$$E = \begin{cases} -u_0 & \text{on walls} \\ 0 & \text{otherwise} \end{cases}$$

Moves of a Polymer

To move a polymer, we use the Bond-Fluctuation-Method (BFM) [21–23] proposed by I. Carmesin and K. Kremer. The BFM is an ergodic algorithm. Therefore, it should be useful at high density in a narrow space. The polymer chain moves on a square lattice (lattice constant $a = 1$). Each monomer occupies $n_m (= 4)$ lattice sites. Each lattice site can only be part of one monomer under self-avoiding-walk (SAW) conditions. The Bond-Fluctuation-Method makes possible fluctuations of the bond length between 2 and $\sqrt{13}$. In other words, the bond can be taken from a set of 36 allowed bond-vectors obtained from the base set

$$\{(2,0),(2,1),(2,2),(3,0),(3,1),(3,2)\}$$

and with symmetry operations of the square lattice.

The procedures of our Monte Carlo simulation are followings

1. To set an initial configuration on the lattice.
2. To select one of the monomers of the polymer at random.

3. To select one of the 4 lattice directions, and to move the selected monomer by 1 lattice constant.
4. If the trial move does not break the SAW conditions, the trial configuration is accepted as a new configuration, otherwise to select a new monomer.
5. To repeat the above procedures 2–4.

This procedure does not generate crossed configurations.

Sampling of Configurations 1

In the Metropolice Method, one chooses a sampling probability $P(x)$ equal to weight $\exp(-\beta U(x))$, where $\beta = 1/kT$ (k denotes the Boltzmann constant), x represents a configuration of the system under consideration with a potential U. It fails to access to configurations x if there exist large barriers between them. Furthermore at low temperatures, the probability is very small, and it is quite difficult to sample enough configurations that are statistically uncorrelated. To overcome these difficulties, the Entropic-Sampling Method [24] has been proposed.

In the Entropic-Sampling Method, one computes the entropy of the system and one performs a sampling simulation using this entropy. Therefore, this method enables us to obtain the Helmholtz free energy. If one performs the simulation with an arbitrary distribution

$$P(x) \propto \exp[-J(E(x))], \tag{1}$$

it is sufficient to impose, along with ergodicity, a detailed balance condition

$$\frac{W(x \to x')}{W(x' \to x)} = \exp\{-[J(E(x')) - J(E(x))]\}, \tag{2}$$

where $W(x \to x')$ is the transition probability from a configuration x to x'. The distribution $P(x)$ will be projected onto the energy E surface.

$$P(E) \propto \Omega(E) \exp[-J(E)] = \exp[S(E)/k - J(E)], \tag{3}$$

where $\Omega(E)$ and $S(E)(=k \ln \Omega(E))$ are the density of states and the entropy for a given E. If $J(E)$ is chosen equal to $S(E)/k$, the distribution of the energy $P(E)$ becomes a flat distribution. Equations (2) and (3) are the main equations upon which this algorithm is based.

A rough estimate of the entropy $S(E)$ is necessary before a long Monte-Carlo simulation can be undertaken. This procedure is briefly summarized

below:

1. Initially $J(E)$ and $S(E)$ are set to zero for all E. Then, one performs a short Monte-Carlo simulation and obtains the histogram $H(E)$ of E.
2. New estimate for $S(E)$ is made as follows

$$S(E)/k = \begin{cases} J(E) & \text{for } H(E) = 0, \\ J(E) + \ln H(E) & \text{otherwise.} \end{cases} \tag{4}$$

3. With such new estimate $J(E)(=S(E)/k)$, one performs a short Monte-Carlo simulation. Trial moves are accepted according to Eq. (2).
4. One repeats the above procedures 2 and 3 until one reaches sampling distribution to approximately flat distribution on the whole range (or a desired range) of energy.
5. Finally, to obtain many desired observables, one performs a long Monte-Carlo simulation with the weight $\exp(-J(E))$, $J(F)$ being one already obtained.

By using above procedures, sampling is possible obeying an approximately flat distribution. Therefore one can not be trapped in energy barriers, and one can obtain almost all the possible equilibrium configurations. Therefore, even for low temperatures, one can sample enough configurations. One of the advantages of this sampling method is to be able to obtain desired observables at arbitrary temperature by a single long simulation. The thermodynamic average $< \mathcal{O} >$ of an observable $\mathcal{O}(x)$ can be estimated by

$$\begin{aligned} < \mathcal{O} > &= \frac{\sum_{i=1}^{n} \mathcal{O}(x_i) P^{-1}(x_i) \exp[-\beta U(x_i)]}{\sum_{i=1}^{n} P^{-1}(x_i) \exp[-\beta U(x_i)]} \\ &= \frac{\sum_{i=1}^{n} \mathcal{O}(x_i) \exp[J(U(x_i)) - \beta U(x_i)]}{\sum_{i=1}^{n} \exp[J(U(x_i)) - \beta U(x_i)]}, \end{aligned} \tag{5}$$

where the sum denotes the simulation over the configurations obtained by the Monte-Carlo simulation with the probabilty function $P(x)$. This Entropic-Sampling Method is essentially the same [30] as Multicanonical Method [25–29].

Sampling of Configurations 2

In Subsection 3.3, we will treat the case of semi-confined space to investigate behaviors and properties of a polymer chain near a wall, *e.g.*, the adsorption

transition *etc.* To execute this, we adopt the following sampling technique. First, one chooses an initial polymer configuration of which at least one monomer is on the wall at bottom, and performs simulations using the Entropic-Sampling Method. However, one prepares an upper-boundary. Provided that at least one monomer touches this upper-boundary, one restarts to sample configurations from the initial configuration. To prepare for an enough space so that the polymer chain could possibly be under no influence of the wall during simulation, one have to choose an appropriate distance between the wall and the upper-boundary d_{up}. Since through each simulation the sequence of random number is succeeded, the 1st move from the initial configuration is usually different at each time. Thus it becomes possible to sample various different configurations. Number of steps neccessary to sample varys upon d_{up}. d_{up} can not be too large for CPU time available.

3. RESULTS

3.1. Isolated Polymer Chain

The radius of gyration Rg is a useful parameter meaning the extent of polymer configurations, and is defined by

$$\begin{aligned} Rg^2 &= \frac{1}{N}\sum_{i=1}^{N} s_i^2 \\ s_i &= \mathbf{r}_i - \mathbf{R}_{\mathbf{G}} \\ \mathbf{R}_{\mathbf{G}} &= \sum_{i=1}^{N} m_i \mathbf{r}_i \Big/ \sum_{i=1}^{N} m_i, \end{aligned} \tag{6}$$

where $\mathbf{R}_{\mathbf{G}}$, $\mathbf{r}_i$ and m_i are the center of mass of the polymer, the position vector and the mass of the i-th monomer, respectively. N denotes the number of monomers of the polymer. All monomer's mass are assumed to have the same one ($m_i = m = \text{const.}$).

According to the Flory theory, the radius of gyration Rg_0 of an isolated linear polymer chain satisfies the following scaling rule for real chains, in which excluded volume interactions are taken into account.

$$\begin{aligned} &< Rg_0^2 > \propto N^{2\nu} \\ &\nu = 3/(d+2) \end{aligned} \tag{7}$$

where d denotes the dimension of the system, and ν denotes the Flory exponent. Flory studied for $d = 3$, and for more generalized d Fisher did.

First, we have performed our simulation for an isolated linear polymer chain for the 2-dimensional case, and obtained the mean square radius of gyration (scaling plot) as a function of number of monomers N in Figure 1. It is found that the scaling rule, Eq. (7), is well satisfied and one can also see a weak isotropic behavior at low N.

As mentioned above, the radius of gyration expresses the extent of the polymer. Therefore it is of interest to study relations between the polymer-length (the monomer numbers) and the diameter of capillary (distance between one wall and another). In Table I, values of the radius of gyration obtained for some monomer numbers are shown. These are helpful to consider parameter settings to our MC simulations in a capillary.

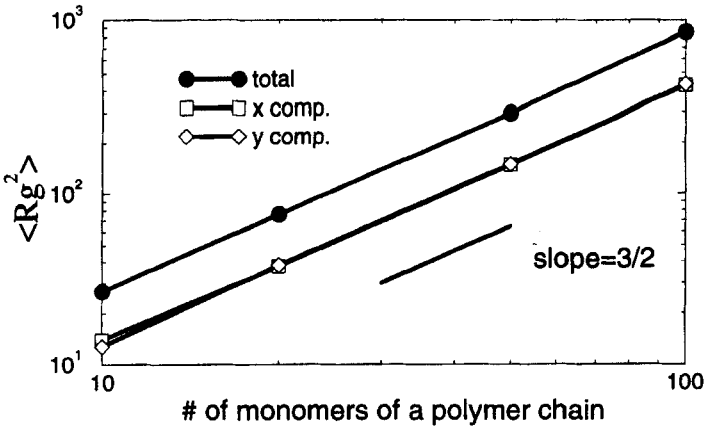

FIGURE 1 Scaling plot for the radius of gyration Rg_0 as a function of number of monomers N for a isolated polymer chain.

TABLE I Values of the radius of gyration Rg_0 for the isolated polymer chain, where N is the number of monomers

N	Rg_{0x}^2	Rg_{0y}^2	Rg_0^2	Rg_0
10	14.0	12.8	26.8	5.18
20	37.6	38.1	75.7	8.70
50	147.3	148.8	296.1	17.21
100	425.3	428.4	853.7	29.22

3.2. Number of Monomers Dependence

In this subsection, a polymer confined in a narrow capillary is considered. To investigate N (the number of monomers) dependence in the capillary, the wall-distance D is fixed at $D = 16$, and monomer numbers are varied.

Characteristics of the system under a thermal equilibrium condition are expressed by thermodynamical functions. Therefore, thermal equilibrium states and stability of the system need to estimate the thermodynamical potential. For this purpose, we need to calculate the Helmholtz free energy F as a function of the radius of gyration chosen as a state variable. We obtained the Helmholtz free energy at four different temperatures for the case of number of monomers $N = 50$, as show in Figure 2. At a high temperature ($kT/u_0 = 0.60$), there is a minimum of Helmholtz free energy F at a small radius of gyration. At a lower temperature ($kT/u_0 = 0.40$), another minimum appears at a larger radius of gyration, and the curve has two local minima for the Helmholtz free energy. At this temperature, two

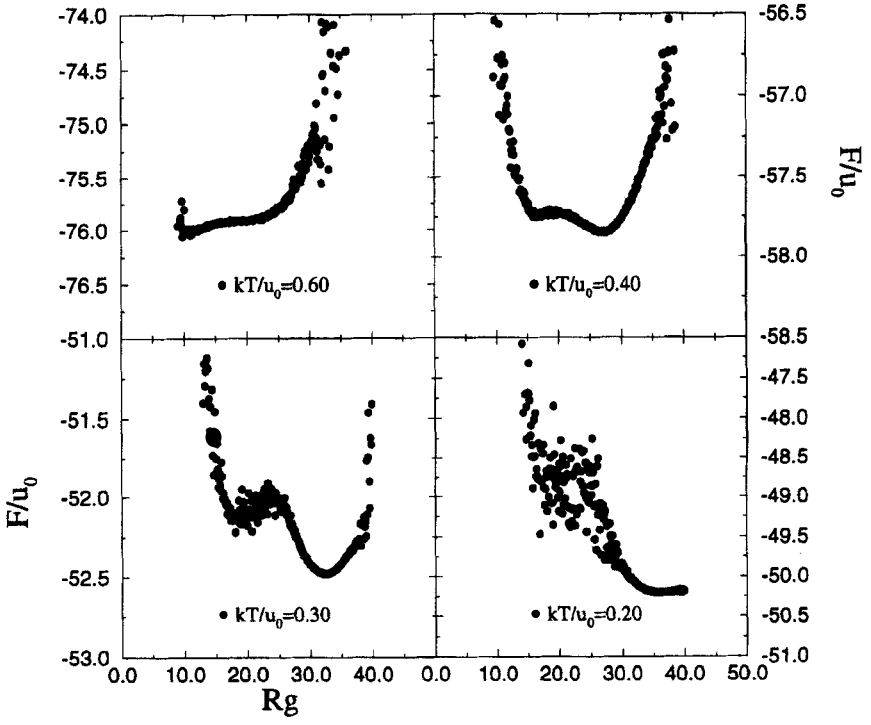

FIGURE 2 The Helmholtz free energy F as a function of the radius of gyration Rg for the wall distance $D = 16$ and the number of monomers $N = 50$.

stable states correspond to configurations with a large radius of gyration and a small one. At lower temperatures, the difference between the values of radius of gyrations at which the Helmholtz free energy indicates local minimum becomes gradually large, moreover the free energy minimum gaps also becomes large, and configurations with large radii of gyration are more stable ($kT/u_0 = 0.30$). At a still lower temperature ($kT/u_0 = 0.20$), there is only one minimum at a larger radius of gyration, and the configurations with large radius of gyration are stable. According to the Helmholtz free energy calculation, it turns out that a specific transition takes place at near $kT/u_0 = 0.40$. The data dispersions at each temperature shown in Figure 2 are caused by low distribution of the radius of gyration (see Fig. 9).

Physical quantities like the specific heat near the transition temperature becomes also characteristic. The temperature dependence of the specific heat Cv is shown in Figure 3. As in response to the free energy, the specific heat becomes characteristic. The peak of the specific heat is seen at nearly the same temperature ($kT/u_0 \simeq 0.39$) irrespective to the number of monomers. In addition to this, a shoulder appears at a lower temperature ($kT/u_0 \leq 0.3$). All these curves look similar qualitatively.

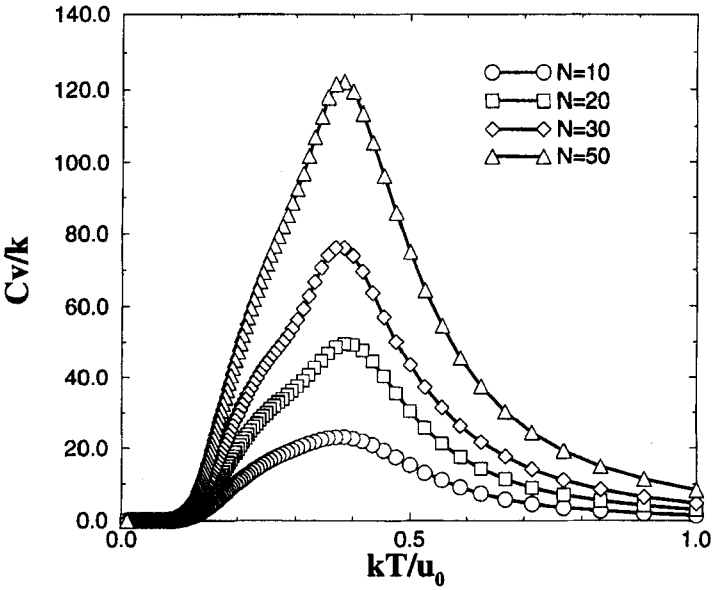

FIGURE 3 The number of monomers N dependence of the specific heat Cv as a function of temperature for the wall distance $D = 16$.

Figure 4 shows the projection of the bond-length Pr(b − 1) to the component perpendicular to the walls (y component) at various temperatures. Denoting the projection operator by $\mathcal{P}$, Pr(b − 1) can be expressed as follows,

$$\begin{aligned} \Pr(\mathrm{b}-1) &\equiv \sum_{i=1}^{N-1} |\mathcal{P}\mathbf{b}_i|/(N-1) \\ &= \sum_{i=1}^{N-1} |r_{i+1y} - r_{iy}|/(N-1) \end{aligned} \tag{8}$$

where $\mathbf{b}_i$ and r_{iy} are the i-th bond-vector and the y-component of the i-th monomer's position vector, respectively. This is an important parameter to estimate predominant configurations at each temperature. Pr(b − 1) vanishes to zero as the temperature decreases for any monomer numbers that we have studied here. Therefore the configurations of the polymers may be all parallel to the walls at very low temperature, unlike coil-like configurations, of which bond-vectors distribute randomly. However Figure 4 does not give us any informations about the distribution of the polymer as a function of the distance from each wall.

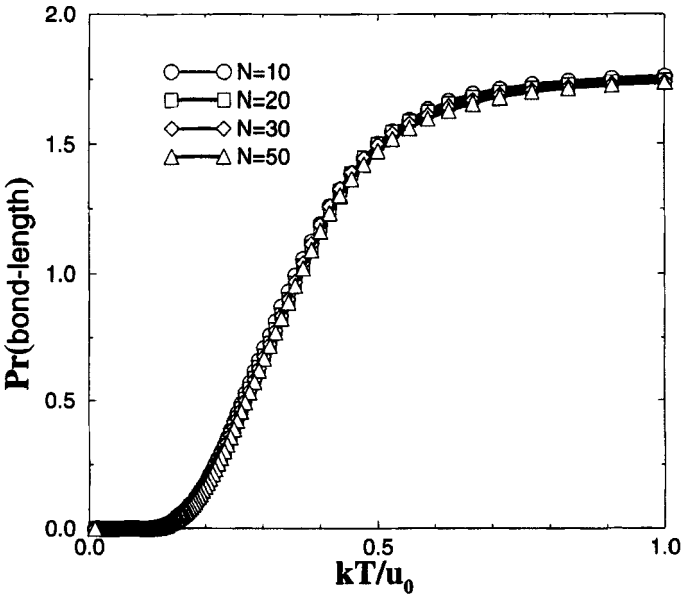

FIGURE 4 The number of monomers N dependence of the projection to axis of parallel to walls of a bond-length Pr(b − 1) as a function of temperature at $D = 16$.

Figure 5 displays the fraction of adsorbed monomers fa as a function of temperature,

$$fa \equiv N_{ad}/N \tag{9}$$

where N_{ad} is number of adsorbed monomers. For our model, this fraction of adsorbed monomers exactly coincides with the energy ratio to the minimum energy E_{min} ($fa = E/E_{min}$). Since fa saturates to $fa = 1.0$ as the temperature decreases, the configurations at very low temperature correspond to the minimum energy. The curves for every monomer numbers give rise to the same one, there is no N dependence.

According to Figures 4 and 5, it is indicated the polymer chain lies on one side wall just like one dimensional adsorption at low temperatures. We can confirm this result with scaling rules of radius of gyration. For the radius of gyration at very low temperature, the only x component has a non-zero value. The scaling rule of the mean square radius of gyration at one dimension describes $Rg^2 \propto N^2$ (see Eq. (7)). We display the square of radius of gyration parallel to the walls divided by N^2, that is $< Rg_x^2 > /N^2$, as a function of temperature in Figure 6. At low temperatures, since the curves for all monomer numbers follow the same, the one-dimensional scaling

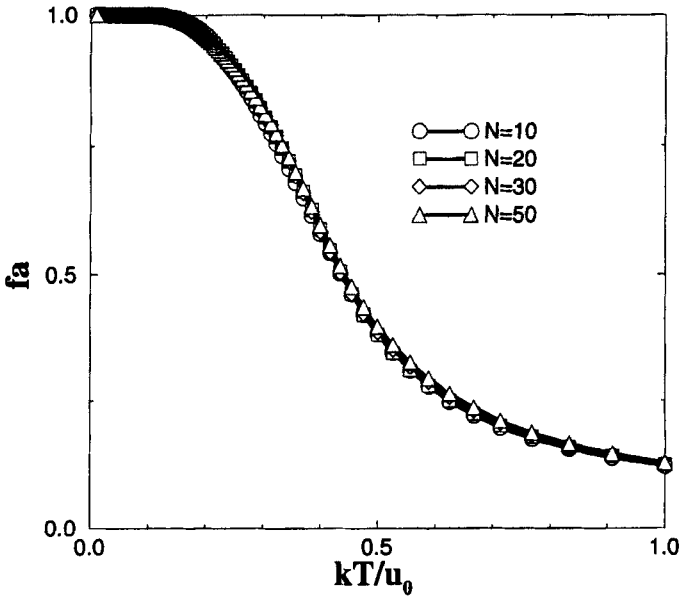

FIGURE 5 The number of monomers N dependence of the fraction of adsorbed monomers fa as a function of temperature at $D = 16$.

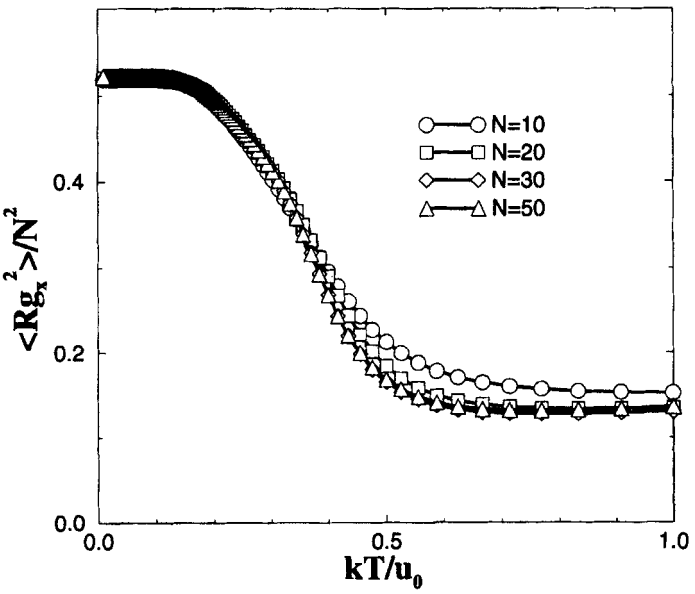

FIGURE 6 The number of monomers N dependence of the x-component radius of gyration parallel to walls as a function of temperature at $D = 16$.

property can be confirmed. In other words, $< Rg_x^2 >$ for a larger number of monomers tends to have a larger value. From the temperature dependence of the radius of gyration perpendicular to the walls (Fig. 7), the peak of the y component of the radius of gyration appears at a higher temperature than that corresponding to the peak of the specific heat ($kT/u_0 \simeq 0.39$, see Fig. 3). This indicates that the polymer chain is pulled to the both side walls. Also it turns out that $< Rg_y^2 >$ vanishes to zero at low temperatures and tends to have larger value for the larger number of monomers.

The space (region) of the capillary is divided into three domains as follows. The first domain is the capillary walls ($y = 0$ and $y = D$), the second domain is the region near the capillary walls ($0 < y \leq \delta$ and $D - \delta \leq y < D$), and rest of the inner capillary, *i.e.*, the center domain of the capillary ($\delta < y < D - \delta$), where δ is arbitrarily chosen to be 3, which exactly equals to the maximum value of the allowed bond-vector component in our Bond-Fluctuation-Method. The probability found monomers $\rho(y)$ as a function of distance from either wall is defined by

$$\rho(y) = [\rho_0(y) + \rho_0(D - y)]/2 \tag{10}$$

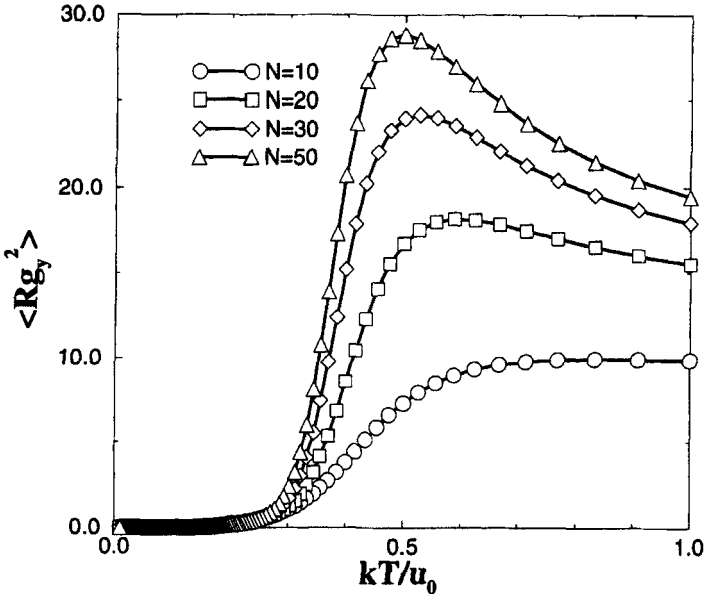

FIGURE 7 Number of monomers N dependence of the y-component radius of gyration perpendicular to walls as a function of temperature at $D = 16$.

$$\rho_0(y) = n(y)/N = \sum_{i=1}^{N} \delta(y - r_{iy})/N \tag{11}$$

where $n(y)$ denotes the number of monomers at the position y, r_{iy} denotes the y component of the i-th monomer, and $\delta(y)$ denotes the Kronecker's delta function. That is, $\rho(y)$ is the normalized value, which is the number of monomers at the distance y from either wall. Because of the mirror symmetry of $\rho(y)$ at $y = D/2$, for the low temperature limit case, it holds that $\lim_{kT/u_0 \to 0}\rho(0) = \lim_{kT/u_0 \to 0}\rho(D) = 0.5$.

For the case of the number of monomers equal to 50 and the distance of walls equal to 16, $\rho(y)$ is shown in Figure 8. Owing to the mirror symmetry at $y = 8$, $\rho(y)$ is only displayed for the half domain of the total width $D = 16$. At an infinite temperature, on account of low entropy (few number of states) near and on the capillary, the probability found monomers on the walls is non-zero small value. At a temperature such as $kT/u_0 \simeq 0.40$, at which the peak of the specific heat takes place (see Fig. 3), the value of $\rho(y)$ at the center region of the capillary ($3 < y \leq 8$) decreases, and at a lower

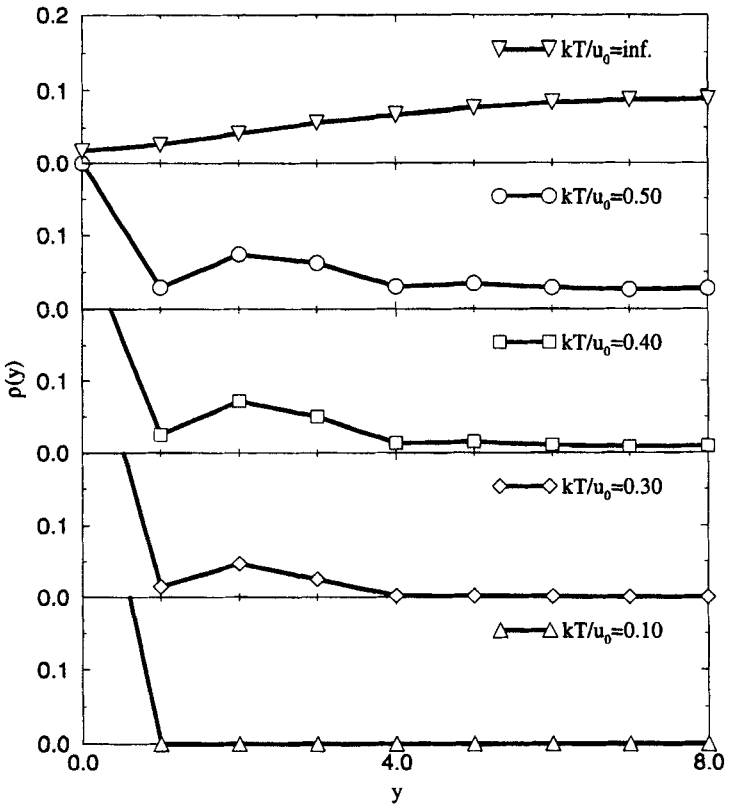

FIGURE 8 The probability of a monomer $\rho(y)$ as a function of distance from either wall for the number of monomers $N = 50$ and the wall distance $D = 16$.

temperature such as $kT/u_0 = 0.30$, the value is non-zero near and on walls only. At $kT/u_0 = 0.10$, $\rho(y)$ equals to zero at any y but on the walls, and since monomers do not exist in the center domain of the capillary, the whole polymer chain lies on either one side of the walls, as indicated in Figures 4 and 5.

Let us now study the distribution of the root square of the radius of gyration $< Rg^2 >^{1/2}$ for the case of the wall distance $D = 16$ at both higher and lower temperatures than that at which the peak of the specific heat appears (see Fig. 9). As the temperature is decreased, the distribution becomes very wide near the transitional temperature. At lower temperatures, the distribution peak shifts to the right (lager Rg), and the distribution becomes sharper. The reason is quite suitable at very low temperature, because Rg becomes larger for one dimensional configurations and the

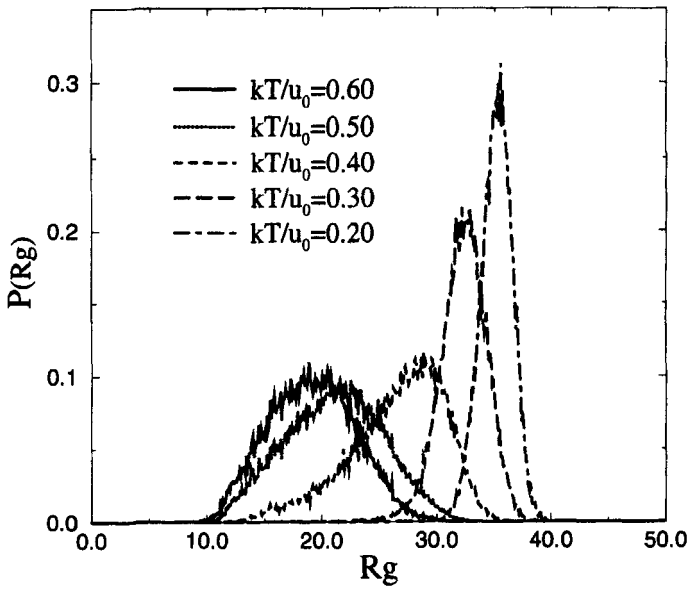

FIGURE 9 The distribution of the radius of gyration $P(Rg)$ for the number of monomers $N = 50$ and the wall distance $D = 16$.

number of possible configurations becomes smaller. Also note that the peak of the distribution of the radius of gyration basically corresponds to the minimum of the free energy at the respective temperature.

We show three snap-shots of characteristic configurations with the corresponding radii of gyration in Figure 10. Configurations (a) are pulled by adsorption to both sides walls, in which the radius of gyration $Rg = 18.06$. Hereafter, such configurations are called "two-wall pulling configurations". (b) shows configurations near and on the one wall, in which the fraction of monomers are adsorbed on the one wall while the other monomers stay away from the wall. The radius of gyration is $Rg = 31.99$. We call such configurations "one-wall-partial adsorption configurations". (c) shows configurations of which all monomers remain on the one wall with the radius of gyration $Rg = 36.22$. We call such configurations "one-wall-full adsorption configurations".

3.3. Adsorption on One Wall

In the previous subsection, we have investigated the influence of the walls on a polymer chain, such as the adsorption transition. In this subsection,

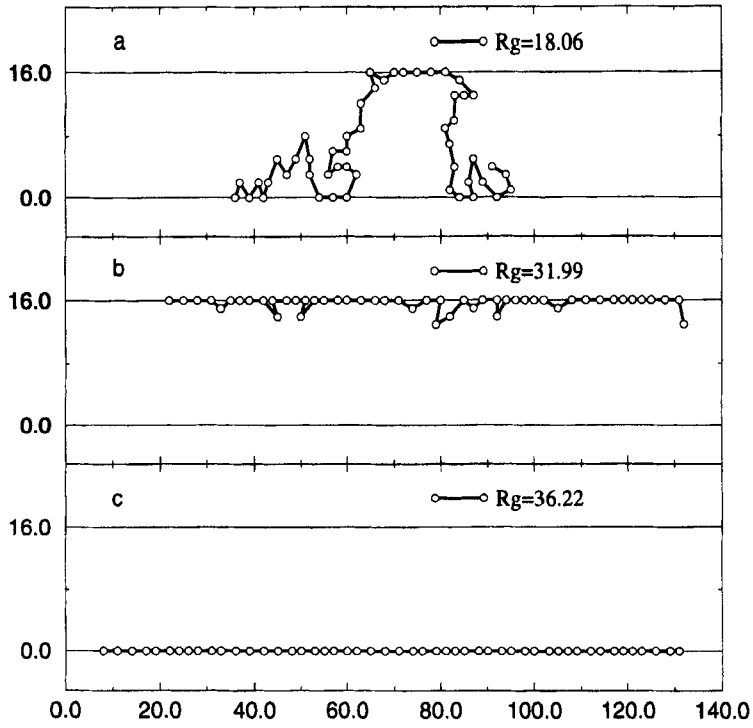

FIGURE 10 Three characteristic configurations (snap-shot) for the number of monomers $N = 50$ and the wall distance $D = 16$. Two parallel lines denote the walls of the capillary.

we will investigate the physical influence of the existence of one wall, for example, a "simple" adsorption transition to the one wall. We use techniques of sampling of configurations mentioned in Section 2. We consider only one wall, and set up the distance d_{up} between the upper-boundary and the bottom wall equal to 100. This satisfies the relationship $d_{up} > 5Rg_0$, where Rg_0 denotes the radius of gyration for an isolated polymer chain, so that the chain can be under no influence of the upper wall during simulation.

The Helmholtz free energy F as a function of the radius of gyration is displayed in Figure 11 for the case of a chain with 50 monomers. In this figure, two local minima are not found clearly. However, the minimum shifts to a larger radius of gyration as the temperature is decreased.

Figure 12 displays the temperature dependence of the specific heat Cv. The peak of the specific heat is seen at almost the same temperature as $kT/u_0 = 0.5$ irrespective to the monomer numbers. As far as the specific heat is

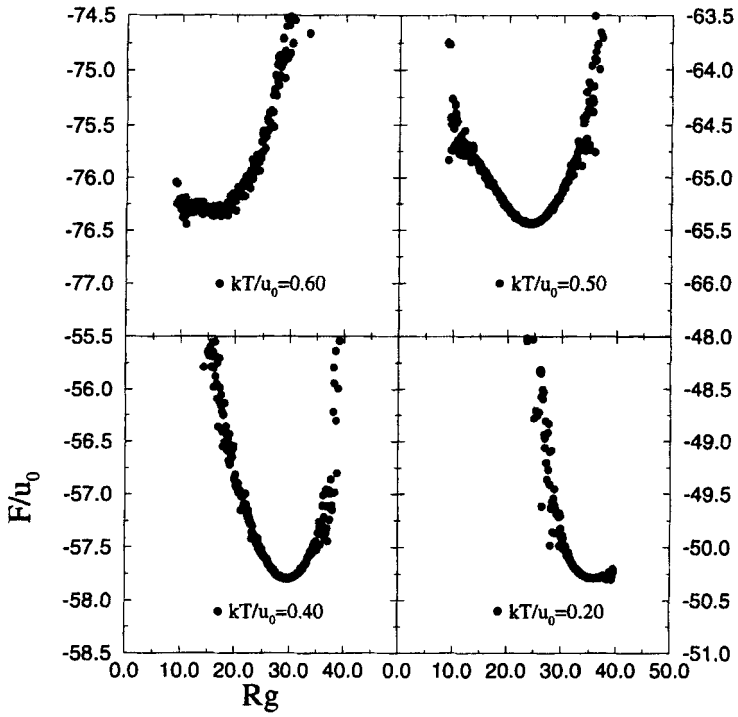

FIGURE 11 The Helmholtz free energy F as a function of the radius of gyration for one-wall system (semi-confined system) for the number of monomers $N = 50$.

concerned, it suggests a transition may occur. However the free energy does not indicate it clearly. So, we should elucidate what happens physically around the temperature at which the peak of the specific heat takes place.

The temperature dependence of the fraction of adsorbed monomers fa is shown in Figure 13. At high temperatures, it is suggestive that chain configurations are not influenced by the wall because all curves vanish to zero. On the other hand, at low temperatures, chains remain on the adsorbing wall and it follows that the system is at the minimum energy state as seen from the fact that $fa = 1.0$.

As already been mentioned in Section 2, fluctuations of the bond length is a characteristic of the Bond-Fluctuation-Method. Figure 14 shows such fluctuations of the bond length as a function of temperature. Since the bond length saturates to 2.50 at low temperatures, it is indicated that the configurations are possibly one dimensional. The reason for this is as follows. Assuming that the configurations are one dimensional, each bond

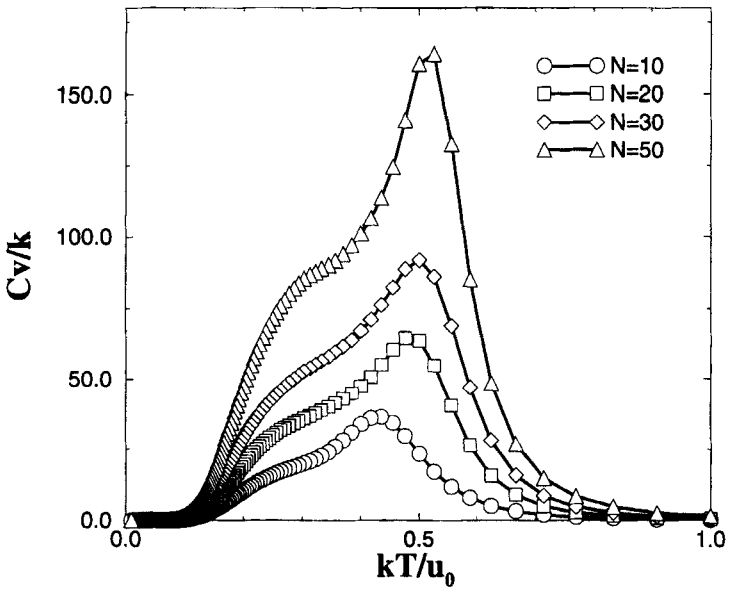

FIGURE 12 The specific heat *Cv* as a function of temperature for one-wall system.

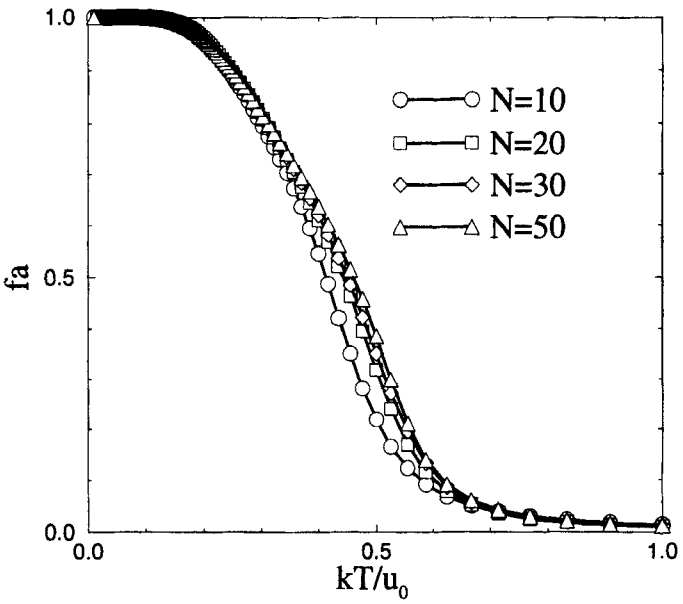

FIGURE 13 The fraction of adsorbed monomers *fa* as a function of temperature for one-wall system.

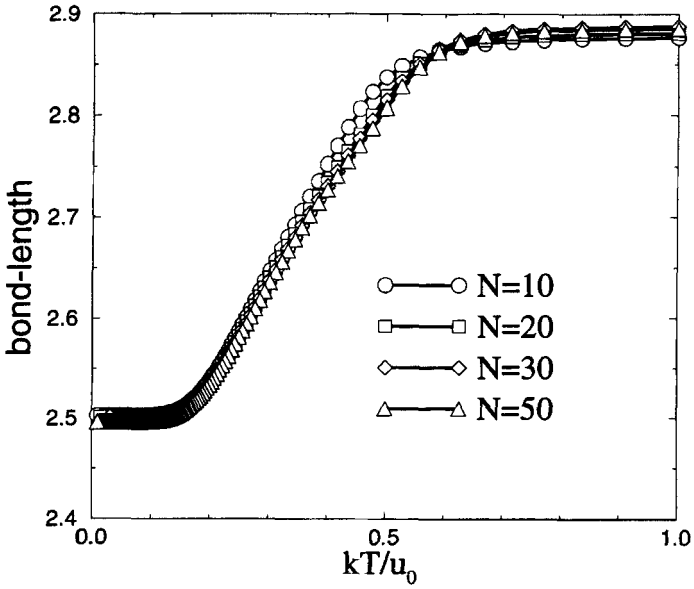

FIGURE 14 The bond-length as a function of temperature for the one-wall system.

length can take 2 or 3 and the number of vectors with either bond length is the same. Therefore, the average of these two possible values of the bond length becomes 2.50. By the same way, one can estimate it at high temperatures as follows. At high temperatures, since the configurations are in coil-states, we can assume that bond vectors are possibly random. This assumption leads to a bond length equal to 2.67 easily. Our Monte Carlo calculations agree very well with these theoretical values.

According to Eq. (7), in the 2-dimensional case the scaling rule for the mean square radius of gyration is written as $Rg^2 \propto N^{3/2}$. Each component of the radius of gyration divided by this two-dimensional scaling, $< Rg_\alpha^2 > /N^{3/2} (\alpha = x, y)$, is shown in Figure 15 as a function of temperature. At high temperatures, it turns out that the configurations are basically isotropic and the scaling rule is well satisfied. This result may indicate that the distance d_{up} between the wall and the upper-boundary used is enough at the present simulation. As the temperature decreases, the x-component increases, while the y-component decreases. According to a suggestion of one-dimensional behavior at low temperatures (see Figs. 13 and 14), the temperature dependence of the component parallel to the wall of the radius of gyration divided by one-dimensional scaling, $< Rg_x^2 > /N^2$, are shown in Figure 16. It turns out that one-dimensional scaling holds very

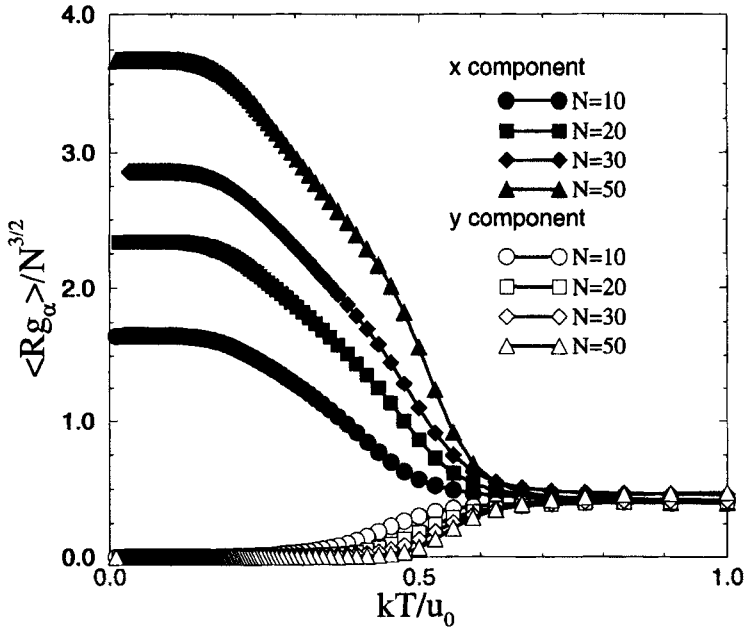

FIGURE 15 The each component of the radius of gyration (Rg_α) as a function of temperature, where $\alpha = x, y$.

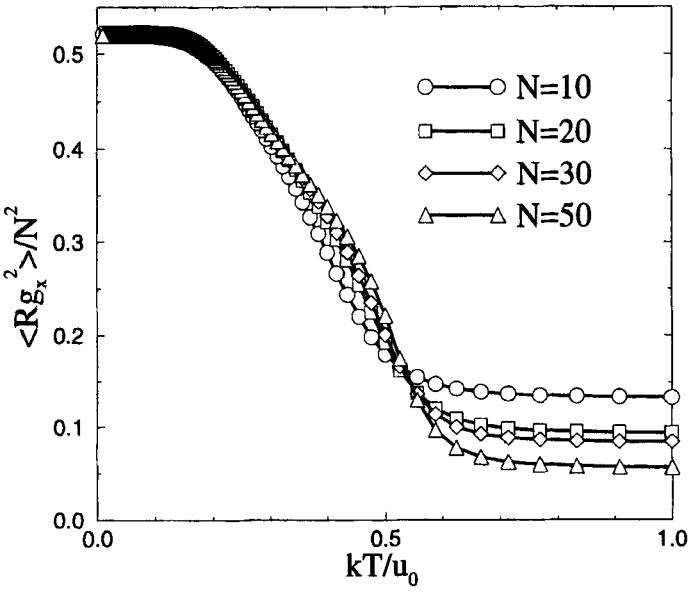

FIGURE 16 The x-component radius of gyration parallel to the wall for one-wall system with one-dimensional scaling.

well at low temperatures, thus the configurations scale with one-dimensional property.

The probability $\rho(y)$ as a function of distance from the wall is displayed in Figure 17, where

$$\rho(y) = \rho_0(y) \tag{12}$$

instead of Eq. (10) because of the lack of the symmetry parallel to the wall. Clearly, at low temperatures, $\rho(y)$ becomes large only on or near the wall.

Figure 18 displays the three characteristic configurations with the corresponding radii of gyration for the polymer chain with 50 monomers. (a) shows the configuration of which no monomer is adsorbed on the wall, and the radius of gyration is $Rg = 17.73$. Therefore, it corresponds to configurations for an isolated polymer chain. We call such configurations

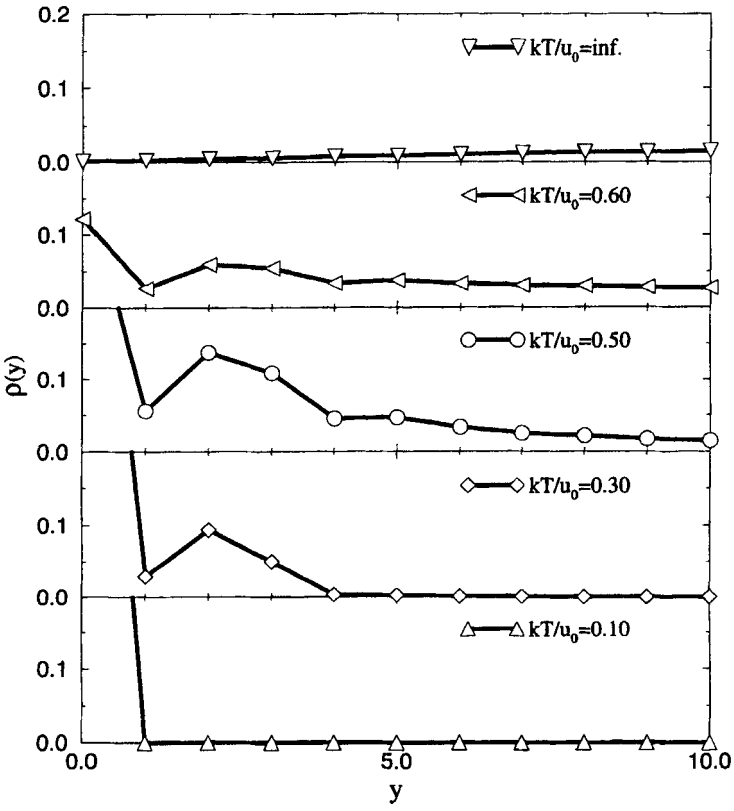

FIGURE 17 The probability of a monomer $\rho(y)$ as a function of distance from the wall.

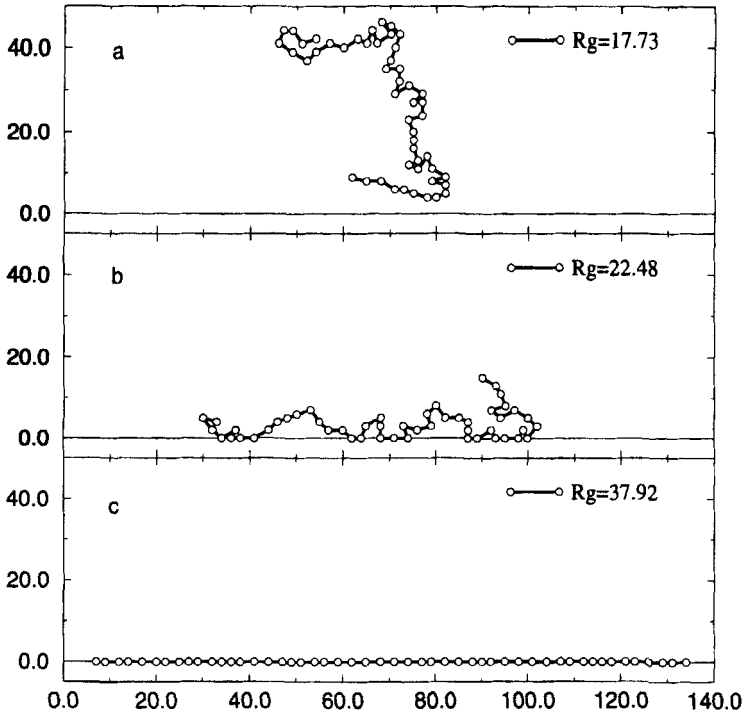

FIGURE 18 Three characteristic configurations (snap-shot) for one-wall system.

"random coil configurations". (b) shows the configuration of which a finite fraction of monomers are adsorbed on the wall, and the radius of gyration is $Rg = 22.48$. This situation is the same as in Figure 10-b. Therefore this is similar to one-wall-partial adsorption configurations. (c) indicates the configuration of which all monomers of the polymer chain remain on the wall, and the radius of gyration is $Rg = 37.92$. This is again one-wall-full adsorption configuration similar to the configuration in Figure 10-c.

In the present model system the total energy of the system increases or decreases only when the monomers adsorb on or disadsorb from the wall(s). In other words, in the "center part area", excepted at least the region away from the walls $d \leq 2Rg_0$ in the case of the confined space with $D \gg 2Rg_0$, each configuration takes the same energy that essentially corresponds to the case of an isolated system. Therefore, if the distance d_{up} between the wall and the upper-boundary is enough, the same result are obtained for different d_{up}'s, in the case of $D \gg 2Rg_0$ with the sampling configuration method 2. The influences of the existence of the one wall that has been obtained so far,

however, can also hold for the two-wall system with $D \gg 2Rg_0$. The transition found in this subsection for one-wall system may be treated as a "simple adsorption" transition.

3.4. Wall-distance Dependence

In order to investigate the wall-distance dependence of the properties of a polymer chain in a capillary, we have carried out similar Monte Carlo calculations to the case studied in the previous subsections, but with a polymer chain with 50 monomers fixed for several different wall distances D's.

For three different wall distances, the Helmholtz free energy as a function of radius of gyration is shown in Figures 19 and 20. Figure 19 is at the temperature $kT/u_0 = 0.40$. Two local minima are observed for every cases, and the gap of the two minima grows as the wall distance becomes larger. Figure 20 displays the Helmholtz free energy at the temperature

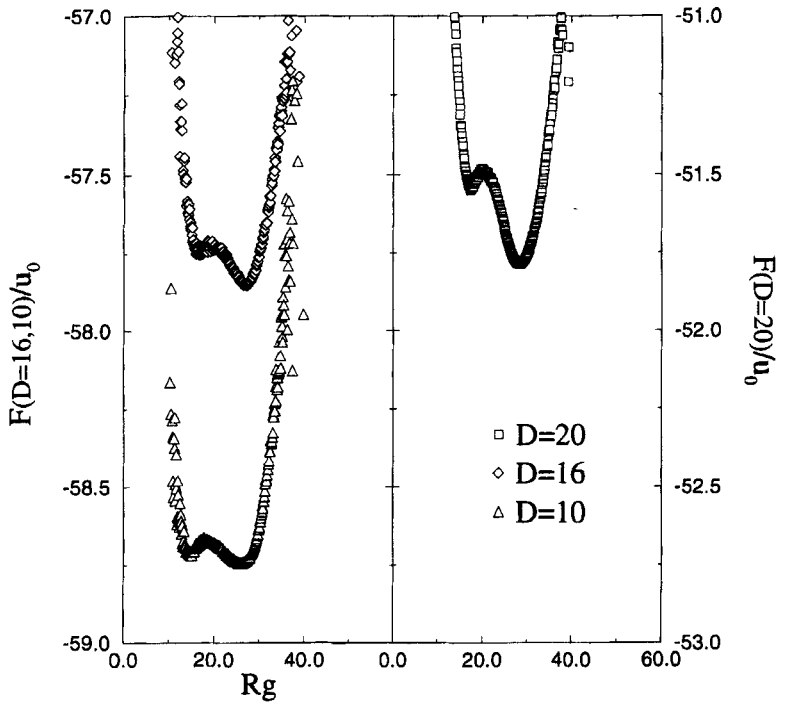

FIGURE 19 The wall-distance D dependence of the Helmholtz free energy F as a function of the radius of gyration of the polymer chain with 50 monomers at the temperature $kT/u_0 = 0.40$.

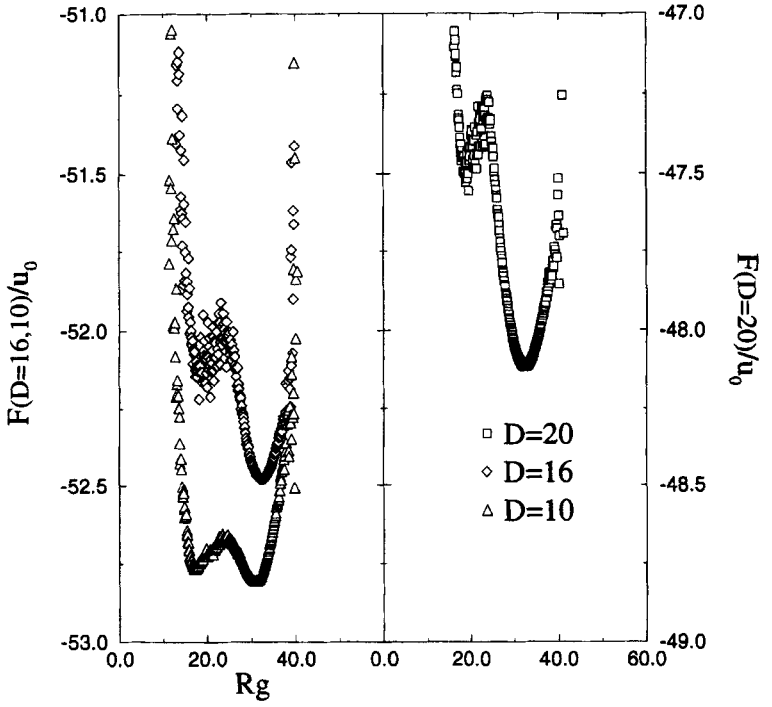

FIGURE 20 The wall-distance D dependence of the Helmholtz free energy F as a function of the radius of gyration of the polymer chain with 50 monomers at temperature $kT/u_0 = 0.30$.

$kT/u_0 = 0.30$. It also turns out that two local minima appear and the gap between these two minima becomes larger as the wall distance becomes wider. Furthermore, the gap of the free energy becomes larger than that at $kT/u_0 = 0.40$. Therefore, it is possible that the gap for a some wall distance becomes the same gap for a narrower wall distance but at a lower temperature.

This property is also related to the specific heat. Figure 21 displays the specific heat Cv at the three different wall distances and for the one-wall system. At high temperatures ($kT/u_0 \geq 0.7$), because of large number of states available to the polymer including wall attachment configurations even for a rather narrower wall distance, the specific heat becomes possibly larger. As the wall distance becomes narrower, the specific heat peak shifts to a lower temperature. This may be interpreted as follows. At high temperatures, when the wall distance decreases, the polymer can be pressed to both directions of walls, so that the energy of the polymer decreases, and the number of monomers of the center region of the capillary decreases.

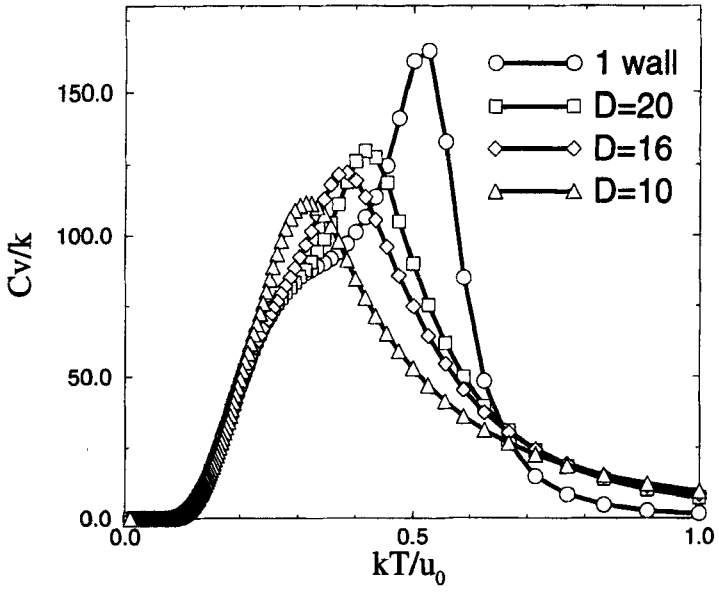

FIGURE 21 The wall-distance D dependent of the specific heat Cv as a function of temperature for the number of monomers $N = 50$.

Because of this situation, it happens that the energy difference on the transition from an adsorpted state on two walls (two-wall pulling configurations) to an adsorpted state on and near the one wall (one-wall-partial adsorption configurations) is small. This also suggests that, the narrower the wall distance becomes, the stronger the forces necessary to tear off monomers adsorbed on one side wall become. At low temperatures, a shoulder appears, and the Cv for different D's does not show any D dependence. This suggests that energy fluctuations are needed to rearrange configurations with a finite fraction of monomers disadsorbed through the effect of the excluded volume interactions to most stable one-dimensional configurations (one-wall-full adsorption configurations). As the wall distance becomes larger and larger, the temperature corresponding to the peak becomes higher, and it approaches the temperature at which the simple adsorption takes places.

The radius of gyration parallel to the walls (x-component) divided by the one-dimensional scaling $< Rg_x^2 > /N^2$ is shown in Figure 22 as a function of temperature for different wall distances. At high temperatures, it becomes larger as two walls are narrower. This implies that the polymer is spread to the direction parallel to the walls. As the temperature is lowered,

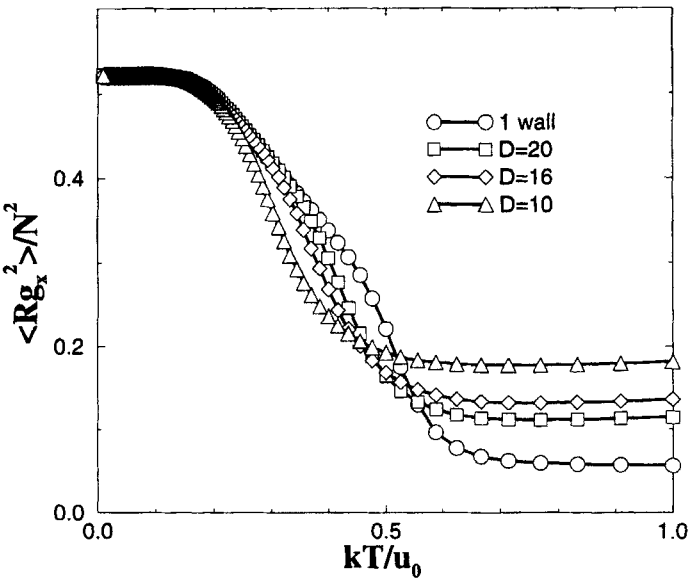

FIGURE 22 The wall-distance D dependence of the x-component radius of gyration parallel to the wall for the number of monomers $N = 50$ with one-dimensional scaling.

$< Rg_x^2 > /N^2$ for a wider wall distance is larger, and thus the wall-distance dependence changes. This can be interpreted as follows. The transition between two-wall pulling configurations and one-wall-partial adsorption configurations takes place at lower temperature as the wall distance becomes narrower. At temperatures lower than the transition temperature, $< Rg_x^2 > /N^2$ becomes large due to the fact that the polymer is confined in a much slender area. At lower temperatures, the x-components of the radii of gyration divided by N^2 becomes nearly the same for all D's not only for the cases of the wall distances $D = 16$ (see Subsection 3.2) and $D \gg Rg_0$ (*e.g.*, simple adsorption, see Subsection 3.3) in which their configurations follow almost as one-dimensional, but also for the cases of the wall distances $D = 10$ and 20. This indicates that the configurations remain on the adsorbed wall (one-wall-full adsorption configurations) irrespective of the wall distance. Also it turns out that near the temperature at which the specific heats become the same for different D's, the x-components of the radii of gyration divided by N^2 become the same as well.

The radius of gyration perpendicular to the wall (y-component) $< Rg_y^2 >$ as a function of temperature for three different wall distances is shown in Figure 23. For low temperatures, the y-component of the radius of gyration

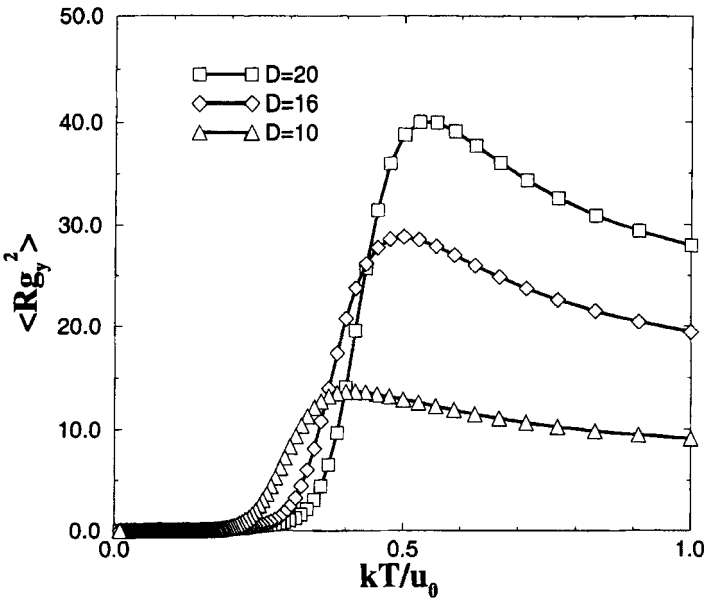

FIGURE 23 The wall-distance D dependence of the y-component radius of gyration perpendicular to the wall for number of monomers $N = 50$.

vanishes to zero, indicating one-wall-full adsorption configurations. For high temperatures, the wider the wall distance becomes, the more the perpendicular-component radius of gyration increase. The peak of $< Rg_y^2 >$ indicates that the polymer is pulled to both sides of walls (two-wall pulling configurations). The temperatures of these peaks are at a higher temperature than the peak of the specific heat (Fig. 21).

Figure 24 shows the fraction of the adsorbed monomers fa at different wall distances. The system is in a minimum energy state at low temperatures since $fa = 1.0$. At high temperatures, fa becomes larger for a narrower wall distance. This is because that when the wall distance is wider, many monomers are found in the center area between two walls, and the number of monomers adsorbed on the walls accordingly decreases.

4. CONCLUSION AND DISCUSSION

In this paper, we have performed Monte Carlo simulations of a single linear polymer chain confined in two parallel impenetrable adsorbing walls. The moves of a polymer obey the Bond-Fluctuation-Method and sampling of

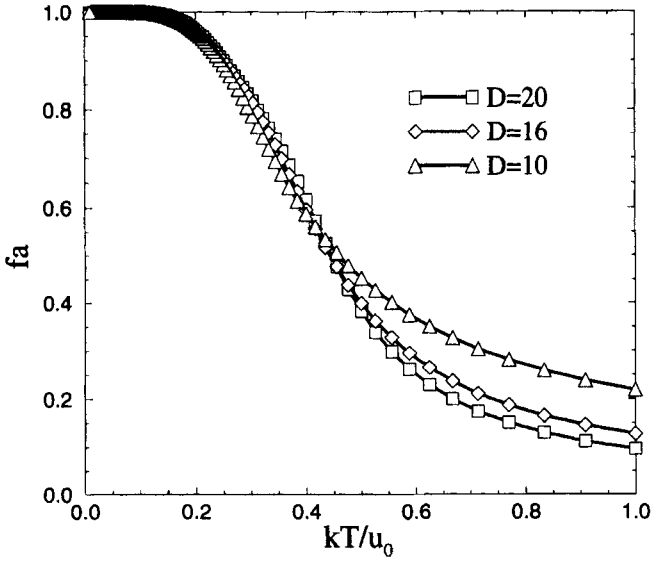

FIGURE 24 The wall-distance D dependence of the fraction of adsorbed monomers fa for the number of monomers $N = 50$.

configurations obeys the Entropic-Sampling Method. We have investigated the influence of the number of monomers of a single polymer at constant wall distance on properties such as specific transitions *etc.* Besides, we have investigated the influence of the wall distance at constant number of monomers.

For the case of constant wall distance, the properties are nearly independent of the number of monomers.

Under the condition that the value of the wall distance roughly equals to the radius of gyration of an isolated polymer, a specific transition has been obtained between two-wall pulling configurations and one-wall-partial adsorption configurations. This transition occurs in monomers away from the two walls by reducing the total energy of the system. This gives rise to the double minimum of the Helmholtz free energy as a function of the radius of gyration and the peak of the specific heat as a function of temperature. At lower temperatures, configurations are rearranged to take in desorbing monomers due to the excluded volume interaction. Another transition takes place between one-wall-partial adsorption configurations and one-wall-full adsorption configurations. This gives rise to the shoulder of the specific heat.

Under the condition that the value of the wall distance is much wider than the radius of gyration of the isolated polymer, the configuration takes

random coil configurations instead of two-wall pulling configurations at high temperatures because no monomers adsorb on either wall. This is reflected in the fact that the partial entropy near the center of the walls is higher than that on or near the walls. The configurations near the center of the walls at low temperature are not filled because of higher free energy. This is consistent with the probability of $\rho(y)$ (see Fig. 17).

As the wall distance decreases at high temperatures, when the wall distance equals to the radius of gyration of the isolated polymer, some monomers of a polymer inevitably touch to the walls so that both walls press the configuration. Therefore, it is proper to assume that the polymer keeps in touch with both walls. We call this configuration "two-wall touch configuration". Though the boundary between random coil configurations and two-wall touch configurations is not in the range of simulation that we have performed in this paper, perhaps the influence of both walls appears under the condition that the wall distance becomes narrower than a maximum of the end-to-end distance (a maximum of the polymer-length) of a polymer ($D \leq Rn_{\max} = l_{\max}$), and the transition between them will occur. The boundary between two-wall touch configurations and two-wall pulling configurations has not been obtained in the present work. However, for the transition between two-wall pulling configurations and one-wall-partial adsorption configurations, the transition temperature shifted to a lower temperature as the wall distance decreases. For the transition between the

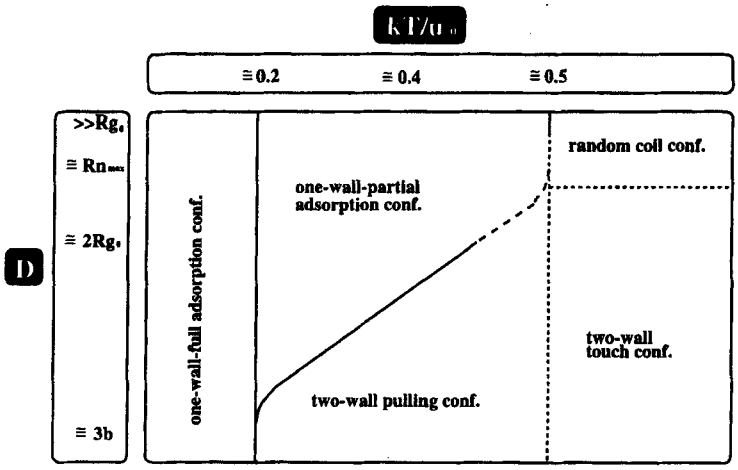

FIGURE 25 The hypothetical diagram for a polymer chain in 2-dimensional parallel walls, where Rg_0, $Rn_{\max}$, b denote an average of the radius of gyration of an isolated polymer chain, a maximum of the end-to-end distance of a polymer chain, and a bond-length of a polymer chain respectively.

one-wall-partial adsorption configurations and one-wall-full adsorption configurations, the transition temperature was independent on the wall distance.

Finally, we summarize the present study mentioned so far by showing a hypothetical diagram for a polymer chain in two-dimensional parallel walls in Figure 25.

Acknowledgement

This study was supported by the Original Industrial Technology R & D Promotion Program from the New Energy and Industrial Technology Development Organization (NEDO).

References

[1] Jorgenson, J. W. and Lukacs, K. D. (1983). "Capillary Zone Electrophoresis", *Science*, **222**, 266.
[2] Lee, K. J. and Heo, G. S. (1991). "Free solution capillary electrophoresis of proteins using untreated fused-dilica capillaries", *J. Chromatogr.*, **559**, 317.
[3] Hjertén, S., Elenbring, K., Kilár, F., Liao, J.-L., Chen, A. J. C., Siebert, C. J. and Zhu, M.-D. (1987). "Carrier-free zone electrophoresis displacement electrophoresis and isoelectric focusing in a high-performance electrophoresis apparatus", *J. Chromatogr.*, **403**, 47.
[4] Kilár, F. and Hjertén, S. (1989). "Fast and high resolution analysis of human serum transferrin by high performance isoelectric focusing in capillaries", *Electrophoresis*, **10**, 23.
[5] Lumpkin, O. J., Déjardin, P. and Zimm, B. H. (1985). "Theory of Gel Electrophoresis of DNA", *Biopolymers*, **24**, 1573.
[6] Hjertén, S. (1987). "High-performance electrophoresis: The electrophoretic counterpart of high-performance liquid chromatography", *J. Chromatogr.*, **270**, 1.
[7] Cohen, A. S. and Karger, B. L. (1987). "High-performance Sodium dodecyl sulfate polyacrylamide gel capillary electrophoresis of peptides and proteins", *J. Chromatogr.*, **397**, 409.
[8] Tsuji, K. (1991). "High-performance capillary electrophoresis of proteins Sodium dodecyl sulphate-polyacrylamide gel-filled capillary column for the determination of recombinant biotechnology-derived proteins", *J. Chromatogr.*, **550**, 823.
[9] Cohen, A. S., Nagarian, D. R., Paulus, A., Guttman, A., Smith, J. A. and Karger, B. L. (1988). "Rapid separation and purification of oligonucleotides by high-performance capillary gel electrophoresis", *Proc. Natl. Acad. Sci. USA*, **85**, 9660.
[10] Guttman, A., Cohen, A. S., Heiger, D. N. and Karger, B. L. (1990). "Analytical and Micropreparative Ultrahigh Resolution of Oligonucleotides by Polyacrylamide Gel High-Performance Capillary Electrophoresis", *Anal. Chem.*, **62**, 137.
[11] Baba, Y. (1993). "Prediction of the behaviour of oligonucleotides in high-performance liquid chromatography and capillary electrophoresis", *J. Chromatogr.*, **618**, 41.
[12] Ganzler, K., Greve, K. S., Cohen, A. S., Karger, B. L., Guttman, A. and Cooke, N. C. (1992). "High-Performance Capillary Electrophoresis of SDS-Protein Complexes Using UV-Transparent Polymer Networks", *Anal. Chem.*, **64**, 2665.
[13] Zhu, M., Hansen, D., Burd, S. and Gannon, F. (1989). "Factors affecting free zone electrophoresis and isoelectric focusing in capillary electrophoresis", *J. Chromatogr.*, **480**, 311.
[14] Strege, M. and Lagu, A. (1991). "Separation of DNA Restriction Fragmants by Capillary Electrophoresis Using Coated Fused Silica Capillaries", *Anal. Chem.*, **63**, 1233.

[15] Lauer, H. H. and McManigill, D. (1986). "Capillary Zone Electrophoresis of Proteins in Untreated Fused Silica Tubing", *Anal. Chem.*, **58**, 166.
[16] Hjertén, S. (1985). "High-peformance electrophoresis elimination of electroendosmosis and solute adsorption", *J. Chromatogr.*, **347**, 191.
[17] Cobb, K. A., Dolnik, V. and Novotny, M. (1990). "Electrophoretic Separations of Proteins in Capillaries with Hydrolytically Stable Surface Structures", *Anal. Chem.*, **62**, 2478.
[18] Stamm, M. (1992). "Polymer Interfaces on a Molecular Scale: Comparison of Techniques and Some Examples", *Adv. Polym. Sci.*, **100**, 357.
[19] Factor, B. J., Russell, T. P. and Toney, M. F. (1993). "Grazing Incidence X-ray Scattering Studies of Thin Films of an Aromatic Polyimide", *Macromolecules*, **26**, 2847.
[20] Jörg, Baschnagel and Kurt Binder (1995). "On the Influence of Hard Walls on Structural Properties in Polymer Glass Simulation", *Macromolecules*, **28**, 6808.
[21] Carmesin, I. and Kremer, K. (1988). "The Bond Fluctuation Method: A New Effective Algorithm for the Dynamics of Polymers in All Spatial Dimensions", *Macromolecules*, **21**, 2819.
[22] Carmesin, I. and Kremer, K. (1990). "Static and dynamic properties of two-dimensional polymer melts", *J. Phys. (Paris)*, **51**, 915.
[23] Kremer, K. and Binder, K. (1988). Monte Carlo Simulations of Lattice Models for Macromolecules", *Computer Phys. Rep.* 7, **6**, 259.
[24] Lee, J. (1993). "New Monte Carlo Algorithm: Entropic Sampling", *Phys. Rev. Lett.*, **71**, 211.
[25] Berg, B. and Neuhaus, T. (1991). "Multicanonical algorithms for first order phase transitions", *Phys. Lett. B*, **267**, 249.
[26] Berg, B. and Neuhaus, T. (1992). "Multicanonical Ensemble: A New Approach to Simulate First-Order Phase Transitions", *Phy. Rev. Lett.*, **68**, 9.
[27] Berg, B. and Celik, T. (1992). "New Approach to Spin-Glass Simulations", *Phys. Rev. Lett.*, **69**, 2292.
[28] Hansmann, U. H. E. and Okamoto, Y. (1994). "Comparative study of multicanonical and simulated annealing algorithms in the protein folding problem", *Physica A*, **212**, 415.
[29] Okamoto, Y. and Hansmann, U. H. E. (1995). "Thermodynamics of Helix-Coil Transitions Studied by Multicanonical Algorithms", *J. Phys. Chem.*, **99**, 11276.
[30] Berg, B., Hansmann, U. H. E. and Okamoto, Y. (1995). "Comment on "Monte Carlo Simulation of a First-Order Transition for Protein Folding"", *J. Phys. Chem.*, **99**, 2236.